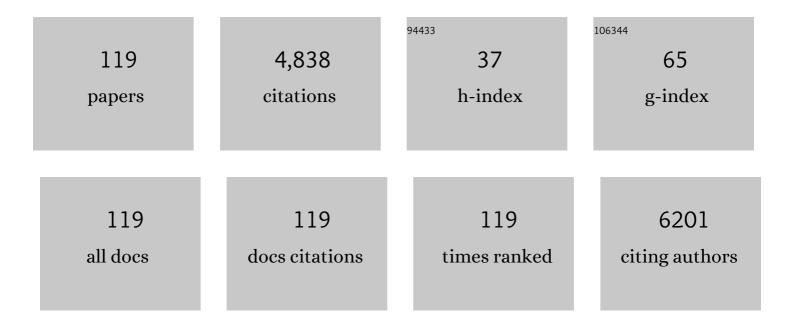
## Xike Tian

## List of Publications by Year in descending order

Source: https://exaly.com/author-pdf/2110604/publications.pdf Version: 2024-02-01



#	Article	IF	CITATIONS
1	Oxygen Vacancy Promoted Heterogeneous Fenton-like Degradation of Ofloxacin at pH 3.2–9.0 by Cu Substituted Magnetic Fe <sub>3</sub> O <sub>4</sub> @FeOOH Nanocomposite. Environmental Science & Technology, 2017, 51, 12699-12706.	10.0	273
2	Promoted peroxymonosulfate activation into singlet oxygen over perovskite for ofloxacin degradation by controlling the oxygen defect concentration. Chemical Engineering Journal, 2019, 359, 828-839.	12.7	213
3	Stable Cu2O nanocrystals grown on functionalized graphene sheets and room temperature H2S gas sensing with ultrahigh sensitivity. Nanoscale, 2013, 5, 1564.	5.6	184
4	Dispersed conductive polymer nanoparticles on graphitic carbon nitride for enhanced solar-driven hydrogen evolution from pure water. Nanoscale, 2013, 5, 9150.	5.6	182
5	A novel singlet oxygen involved peroxymonosulfate activation mechanism for degradation of of of of of of of of of official communications, 2017, 53, 6589-6592.	4.1	154
6	Surface Facet of CuFeO <sub>2</sub> Nanocatalyst: A Key Parameter for H <sub>2</sub> O <sub>2</sub> Activation in Fenton-Like Reaction and Organic Pollutant Degradation. Environmental Science & Technology, 2018, 52, 6518-6525.	10.0	150
7	Nonenzymatic electrochemical sensor based on CuO-TiO2 for sensitive and selective detection of methyl parathion pesticide in ground water. Sensors and Actuators B: Chemical, 2018, 256, 135-142.	7.8	137
8	Biogenic manganese oxide: An efficient peroxymonosulfate activation catalyst for tetracycline and phenol degradation in water. Chemical Engineering Journal, 2018, 352, 469-476.	12.7	129
9	Cr(VI) reduction and immobilization by novel carbonaceous modified magnetic Fe3O4/halloysite nanohybrid. Journal of Hazardous Materials, 2016, 309, 151-156.	12.4	126
10	Polyethylenimine functionalized halloysite nanotubes for efficient removal and fixation of Cr (VI). Microporous and Mesoporous Materials, 2015, 207, 46-52.	4.4	120
11	Highly sensitive and selective paper sensor based on carbon quantum dots for visual detection of TNT residues in groundwater. Sensors and Actuators B: Chemical, 2017, 243, 1002-1009.	7.8	114
12	Enhanced peroxymonosulfate activation for phenol degradation over MnO2 at pH 3.5–9.0 via Cu(II) substitution. Journal of Hazardous Materials, 2018, 360, 303-310.	12.4	111
13	Reductive leaching of manganese from low-grade manganese dioxide ores using corncob as reductant in sulfuric acid solution. Hydrometallurgy, 2010, 100, 157-160.	4.3	108
14	Controlled synthesis of dandelion-like NiCo2O4 microspheres and their catalytic performance for peroxymonosulfate activation in humic acid degradation. Chemical Engineering Journal, 2018, 331, 144-151.	12.7	107
15	Enhanced 2, 4-dichlorophenol degradation at pH 3–11 by peroxymonosulfate via controlling the reactive oxygen species over Ce substituted 3D Mn2O3. Chemical Engineering Journal, 2019, 355, 448-456.	12.7	105
16	Carbon doped molybdenum disulfide nanosheets stabilized on graphene for the hydrogen evolution reaction with high electrocatalytic ability. Nanoscale, 2016, 8, 1676-1683.	5.6	88
17	Facile synthesis of α-MnO2 nanorods for high-performance alkaline batteries. Journal of Physics and Chemistry of Solids, 2010, 71, 258-262.	4.0	82
18	An investigation on the use of electrolytic manganese residue as filler in sulfur concrete. Construction and Building Materials, 2014, 73, 305-310.	7.2	79

XIKE TIAN

#	Article	IF	CITATIONS
19	Facile synthesis of α-MnO2 nanostructures for supercapacitors. Materials Research Bulletin, 2009, 44, 2062-2067.	5.2	71
20	Facile synthesis of Fe 3 O 4 nanoparticles decorated on 3D graphene aerogels as broad-spectrum sorbents for water treatment. Applied Surface Science, 2016, 369, 11-18.	6.1	69
21	Fluoride removal by ordered and disordered mesoporous aluminas. Microporous and Mesoporous Materials, 2014, 197, 156-163.	4.4	65
22	Copper in LaMnO3 to promote peroxymonosulfate activation by regulating the reactive oxygen species in sulfamethoxazole degradation. Journal of Hazardous Materials, 2021, 411, 125163.	12.4	65
23	Polyethylenimine-Functionalized Corn Bract, an Agricultural Waste Material, for Efficient Removal and Recovery of Cr(VI) from Aqueous Solution. Journal of Agricultural and Food Chemistry, 2017, 65, 7153-7158.	5.2	64
24	Heterogeneous Fenton-like degradation of ofloxacin over a wide pH range of 3.6–10.0 over modified mesoporous iron oxide. Chemical Engineering Journal, 2017, 328, 397-405.	12.7	64
25	Successful synthesis of 3D CoSe2 hollow microspheres with high surface roughness and its excellent performance in catalytic hydrogen evolution reaction. Chemical Engineering Journal, 2017, 321, 105-112.	12.7	63
26	Large-Scale Synthesis of Graphene-Like MoSe <sub>2</sub> Nanosheets for Efficient Hydrogen Evolution Reaction. Journal of Physical Chemistry C, 2017, 121, 1974-1981.	3.1	62
27	Fabrication, performance and mechanism of MgO meso-/macroporous nanostructures for simultaneous removal of As( <scp>iii</scp> ) and F in a groundwater system. Environmental Science: Nano, 2016, 3, 1416-1424.	4.3	61
28	Fabrication and structural characterization of porous tungsten oxide nanowires. Nanotechnology, 2005, 16, 2647-2650.	2.6	60
29	Highly selective and sensitive determination of copper ion based on a visual fluorescence method. Sensors and Actuators B: Chemical, 2017, 240, 66-75.	7.8	59
30	Novel MoSe <sub>2</sub> hierarchical microspheres for applications in visible-light-driven advanced oxidation processes. Nanoscale, 2015, 7, 19970-19976.	5.6	57
31	A portable logic detector based on Eu-MOF for multi-target, on-site, visual detection of Eu3+ and fluoride in groundwater. Sensors and Actuators B: Chemical, 2020, 324, 128641.	7.8	56
32	Well-dispersed magnetic iron oxide nanocrystals on sepiolite nanofibers for arsenic removal. RSC Advances, 2015, 5, 25236-25243.	3.6	50
33	pH-dependent oxidation mechanisms over FeCu doped g-C3N4 for ofloxacin degradation via the efficient peroxymonosulfate activation. Journal of Cleaner Production, 2021, 315, 128207.	9.3	50
34	Superior capability of MgAl2O4 for selenite removal from contaminated groundwater during its reconstruction of layered double hydroxides. Separation and Purification Technology, 2017, 176, 66-72.	7.9	46
35	Effect of anionic surfactant inhibition on sewage treatment by a submerged anaerobic membrane bioreactor: Efficiency, sludge activity and methane recovery. Chemical Engineering Journal, 2017, 315, 83-91.	12.7	45
36	Facile synthesis of hierarchical dendrite-like structure iron layered double hydroxide nanohybrids for effective arsenic removal. Chemical Communications, 2016, 52, 11955-11958.	4.1	40

#	Article	IF	CITATIONS
37	Studies of the reduction mechanism of selenium dioxide and its impact on the microstructure of manganese electrodeposit. Electrochimica Acta, 2011, 56, 8305-8310.	5.2	39
38	Ratiometric fluorescence detection of mercuric ions by sole intrinsic dual-emitting gold nanoclusters. Sensors and Actuators B: Chemical, 2019, 278, 82-87.	7.8	37
39	New Insight into a Fenton-like Reaction Mechanism over Sulfidated β-FeOOH: Key Role of Sulfidation in Efficient Iron(III) Reduction and Sulfate Radical Generation. Environmental Science & Technology, 2022, 56, 5542-5551.	10.0	35
40	Novel Colorimetric Method for Simultaneous Detection and Identification of Multimetal Ions in Water: Sensitivity, Selectivity, and Recognition Mechanism. ACS Omega, 2019, 4, 5915-5922.	3.5	34
41	Fabrication and stabilization of nanocrystalline ordered mesoporous MgO–ZrO2 solid solution. Microporous and Mesoporous Materials, 2011, 143, 357-361.	4.4	33
42	Design and synthesis of a molecule with aggregation-induced emission effects and its application in the detection of arsenite in groundwater. Journal of Materials Chemistry C, 2017, 5, 3669-3672.	5.5	32
43	A versatile logic detector and fluorescent film based on Eu-based MOF for swift detection of formaldehyde in solutions and gas phase. Journal of Hazardous Materials, 2021, 410, 124624.	12.4	32
44	Impact of water characteristics on the bioenergy recovery from sewage treatment by anaerobic membrane bioreactor via a comprehensive study on the response of microbial community and methanogenic activity. Energy, 2017, 139, 459-467.	8.8	31
45	Portable ratiometric probe based on the use of europium(III) coordination polymers doped with carbon dots for visual fluorometric determination of oxytetracycline. Mikrochimica Acta, 2020, 187, 125.	5.0	31
46	High-Density, Aligned SiO2Nanowire Arrays:Â Microscopic Imaging of the Unique Growth Style and Their Ultraviolet Light Emission Properties. Journal of Physical Chemistry B, 2006, 110, 15724-15728.	2.6	30
47	Efficient methanogenic degradation of alcohol ethoxylates and microbial community acclimation in treatment of municipal wastewater using a submerged anaerobic membrane bioreactor. Bioresource Technology, 2017, 226, 181-190.	9.6	30
48	Efficient fenton-like degradation of ofloxacin over bimetallic Fe–Cu@Sepiolite composite. Chemosphere, 2020, 257, 127209.	8.2	30
49	Smartphone as a simple device for visual and on-site detection of fluoride in groundwater. Journal of Hazardous Materials, 2021, 411, 125182.	12.4	30
50	Broad-spectrum pesticide screening by multiple cholinesterases and thiocholine sensors assembled high-throughput optical array system. Journal of Hazardous Materials, 2021, 402, 123830.	12.4	29
51	Mechanism for <i>α</i> -MnO <sub>2</sub> Nanowire-Induced Cytotoxicity in Hela Cells. Journal of Nanoscience and Nanotechnology, 2010, 10, 397-404.	0.9	28
52	Safe and efficient degradation of metronidazole using highly dispersed β-FeOOH on palygorskite as heterogeneous Fenton-like activator of hydrogen peroxide. Chemosphere, 2019, 236, 124367.	8.2	28
53	Construction of multi-channel fluorescence sensor array and its application for accurate identification and sensitive quantification of multiple metal ions. Sensors and Actuators B: Chemical, 2020, 303, 127277.	7.8	28
54	Synthesis and electrochemical properties of two types of highly ordered mesoporous MnO2. Electrochimica Acta, 2010, 55, 1682-1686.	5.2	27

#	Article	IF	CITATIONS
55	Manipulation of the Morphology of CdSe Nanostructures: The Effect of Si. Advanced Functional Materials, 2006, 16, 661-666.	14.9	26
56	Recovery of iron oxide concentrate from high-sulfur and low-grade pyrite cinder using an innovative beneficiating process. Hydrometallurgy, 2010, 104, 241-246.	4.3	26
57	Adsorption behavior of methylene blue on amine-functionalized ordered mesoporous alumina. Journal of Porous Materials, 2015, 22, 147-155.	2.6	26
58	Hydroxyl Radical-Involving <i>p</i> -Nitrophenol Oxidation during Its Reduction by Nanoscale Sulfidated Zerovalent Iron under Anaerobic Conditions. Environmental Science & Technology, 2021, 55, 2403-2410.	10.0	26
59	Visual and quantitative detection of glucose based on the intrinsic peroxidase-like activity of CoSe2/rGO nanohybrids. Sensors and Actuators B: Chemical, 2017, 245, 221-229.	7.8	25
60	Enhanced usage of visible light by BiSex for photocatalytic degradation of methylene blue in water via the tunable band gap and energy band position. Journal of Cleaner Production, 2018, 171, 538-547.	9.3	25
61	Novel Erythrocyte-like Graphene Microspheres with High Quality and Mass Production Capability via Electrospray Assisted Self-Assembly. Scientific Reports, 2013, 3, 3327.	3.3	23
62	A ratiometric fluorescence nanosensor for highly selective and sensitive detection of selenite. Analyst, The, 2016, 141, 4685-4693.	3.5	23
63	A promising method for diabetes early diagnosis via sensitive detection of urine glucose by Fe Pd/rGO. Dyes and Pigments, 2019, 164, 20-26.	3.7	23
64	Hierarchical BiOCl microspheres with narrow band gap as visible light active photocatalysts. Inorganica Chimica Acta, 2016, 439, 123-129.	2.4	21
65	Identification and manipulation of active centers on perovskites to enhance catalysis of peroxymonosulfate for degradation of emerging pollutants in water. Journal of Hazardous Materials, 2022, 424, 127384.	12.4	21
66	Low-temperature synthesis and structural characterization of single-crystalline tungsten oxide nanorods. Materials Letters, 2007, 61, 1718-1721.	2.6	20
67	Preparation and tunable photoluminescence of alloyed CdSxSe1â <sup>~,</sup> x nanorods. Journal of Materials Science, 2009, 44, 3015-3019.	3.7	20
68	Visible-light-responsive t-Se nanorod photocatalysts: synthesis, properties, and mechanism. RSC Advances, 2015, 5, 45165-45171.	3.6	20
69	Selective and sensitive colorimetric detection of copper ions based on anti-aggregation of the glutathione-induced aggregated gold nanoparticles and its application for determining sulfide anions. RSC Advances, 2013, 3, 21424.	3.6	19
70	More reactive oxygen species generation facilitated by highly dispersed bimodal gold nanoparticle on the surface of Bi2WO6 for enhanced photocatalytic degradation of ofloxacin in water. Chemosphere, 2021, 269, 128717.	8.2	19
71	Sensitive determination of hardness and fluoride in ground water by a hybrid nanosensor based on aggregation induced FRET on and off mechanism. Sensors and Actuators B: Chemical, 2018, 262, 522-530.	7.8	18
72	Surface acidity and basicity of Mg/Al hydrotalcite for 2, 4-dichlorophenoxyacetic acid degradation with ozone: Mineralization, mechanism, and implications to practical water treatment. Journal of Hazardous Materials, 2021, 402, 123475.	12.4	18

#	Article	IF	CITATIONS
73	Anionic ligands driven efficient ofloxacin degradation over LaMnO3 suspended particles in water due to the enhanced peroxymonosulfate activation. Chemical Engineering Journal, 2022, 427, 130998.	12.7	17
74	Synthesis and growth mechanism: A novel comb-like ZnO nanostructure. Physica E: Low-Dimensional Systems and Nanostructures, 2006, 31, 213-217.	2.7	16
75	Impact of food to microorganism ratio and alcohol ethoxylate dosage on methane production in treatment of low-strength wastewater by a submerged anaerobic membrane bioreactor. Frontiers of Environmental Science and Engineering, 2017, 11, 1.	6.0	16
76	Fe3O4@S-doped ZnO: A magnetic, recoverable, and reusable Fenton-like catalyst for efficient degradation of ofloxacin under alkaline conditions. Environmental Research, 2020, 186, 109626.	7.5	16
77	Significant enhancement of photo-Fenton degradation of ofloxacin over Fe-Dis@Sep due to highly dispersed FeC6 with electron deficiency. Science of the Total Environment, 2020, 723, 138144.	8.0	16
78	Exfoliation of kaolinite by urea-intercalation precursor and microwave irradiation assistance process. Frontiers of Earth Science, 2007, 1, 26-29.	0.5	15
79	Carbon dots–MnO <sub>2</sub> nanocomposites for As( <scp>iii</scp> ) detection in groundwater with high sensitivity and selectivity. Analytical Methods, 2020, 12, 5572-5580.	2.7	15
80	Potassium cation induced controllable synthesis of CAN zeolite hollow microspheres. Microporous and Mesoporous Materials, 2016, 225, 365-370.	4.4	14
81	Insight into bicarbonate involved efficient heterogeneous Fenton-like degradation of sulfamethoxazole over a CuFeO <sub>2</sub> based composite under alkaline conditions. Environmental Science: Nano, 0, , .	4.3	14
82	Synthesis of crystalline ordered mesoporous CaO–ZrO2 solid solution as a promising solid base. Materials Chemistry and Physics, 2010, 124, 744-747.	4.0	13
83	Surface deep oxidation of ofloxacin and 2,4-dichlorophenol over ferrocene@sepiolite due to their synergistic effect in visible light driven heterogeneous Fenton reaction process. Environmental Science: Nano, 2018, 5, 1943-1950.	4.3	13
84	Sulfur quantum dot-based portable paper sensors for fluorometric and colorimetric dual-channel detection of cobalt. Journal of Materials Science, 2021, 56, 4782-4796.	3.7	13
85	Rapid and sensitive screening of multiple polycyclic aromatic hydrocarbons by a reusable fluorescent sensor array. Journal of Hazardous Materials, 2022, 424, 127694.	12.4	12
86	Sensitive and selective ratiometric nanosensors for visual detection of Cu2+ based on ions promoted oxidation reaction. Sensors and Actuators B: Chemical, 2017, 247, 139-145.	7.8	11
87	A carbon-dot-based dual-emission probe for ultrasensitive visual detection of copper ions. New Journal of Chemistry, 2018, 42, 19771-19778.	2.8	11
88	Chemical vapor deposition synthesis and photoluminescence properties of ZnS hollow microspheres. Materials Research Bulletin, 2008, 43, 1966-1970.	5.2	10
89	A simple technique for the facile synthesis of novel crystalline mesoporous ZrO2–Al2O3 hierarchical nanostructures with high lead (II) ion absorption ability. Applied Surface Science, 2013, 284, 412-418.	6.1	10
90	Silica-embedded CdTe quantum dots functionalized with rhodamine derivative for instant visual detection of ferric ions in aqueous media. Journal of Photochemistry and Photobiology A: Chemistry, 2019, 372, 140-146.	3.9	10

#	Article	IF	CITATIONS
91	Natural alumina/silica suspended particles in water to enhance ofloxacin degradation with UVA-H2O2 driven by surface chemistry. Journal of Hazardous Materials, 2021, 412, 125259.	12.4	10
92	Film-based fluorescent sensor for visual monitoring and efficient removal of aniline in solutions and gas phase. Journal of Hazardous Materials, 2022, 435, 129016.	12.4	10
93	Synthesis of Chromium-Doped Malayaite Pigments from Wastewater Containing Low Chromium(VI). Journal of the Air and Waste Management Association, 2010, 60, 1257-1261.	1.9	9
94	Construction of salicylaldehyde analogues as turn-on fluorescence probes and their electronic effect on sensitive and selective detection of As( <scp>v</scp> ) in groundwater. Analytical Methods, 2019, 11, 955-964.	2.7	9
95	Characterization of the effect of surfactant on biomass adaptation and microbial community in sewage treatment by anaerobic membrane bioreactor. Journal of Industrial and Engineering Chemistry, 2019, 76, 268-276.	5.8	9
96	Insight into enhanced Fenton-like degradation of antibiotics over CuFeO2 based nanocomposite: To improve the utilization efficiency of OH/O2- via minimizing its migration distance. Chemosphere, 2022, 294, 133743.	8.2	9
97	Formation of CuS pineal microspheres via a pyridine-solvothermal process. Journal Wuhan University of Technology, Materials Science Edition, 2010, 25, 459-463.	1.0	8
98	Portable smartphone-integrated paper sensors for fluorescence detection of As(III) in groundwater. Royal Society Open Science, 2020, 7, 201500.	2.4	8
99	Selective temperature physical vapor deposition route to tri(8-hydroquinoline)aluminum nanowires, nanowalls, nanoclusters and micro-spherical chains. Solid State Communications, 2006, 138, 530-533.	1.9	7
100	Synthesis and characterization of amoxicillin nanostructures. Nanomedicine: Nanotechnology, Biology, and Medicine, 2005, 1, 323-325.	3.3	6
101	Synthesis of Flower-Like CuS Nanostructured Microspheres Using Poly(ethylene glycol) 200 as Solvent. Journal of Nanoscience and Nanotechnology, 2010, 10, 7770-7773.	0.9	6
102	A mesoporous Pt-SBA-15 nano architecture with catalytic functions on oxidation of CO. Journal of Porous Materials, 2011, 18, 31-35.	2.6	5
103	A Template-Based Electrochemical Method for the Synthesis of High Dense Nickel Nanotube Arrays. Journal of Nanoscience and Nanotechnology, 2007, 7, 673-676.	0.9	4
104	Capturing and storage of CO2 by micron-nano minerals: Evidence from the nature. Diqiu Huaxue, 2011, 30, 569-575.	0.5	4
105	Hierarchical BiOCl Hollow Microspheres Assembled by Ultrathin Nanosheets with Large Surface Area for the Exceptional Visible Light Photocatalytic Activity. Journal of Nanoscience and Nanotechnology, 2017, 17, 6328-6336.	0.9	4
106	Novel AlEgens with a 3,5-dibromobenzaldehyde skeleton: molecular design, synthesis, tunable emission and detection application. Analytical Methods, 2018, 10, 5486-5492.	2.7	4
107	Preparation of ultrafine particles of azithromycin by sonochemical method. Nanomedicine: Nanotechnology, Biology, and Medicine, 2007, 3, 86-88.	3.3	3
108	Tuning the optical properties of alloyed CdSexS1â^'x nanoparticles by changing the constituent stoichiometry. Materials Letters, 2007, 61, 4857-4860.	2.6	3

#	Article	IF	CITATIONS
109	Catalyst-Enhanced Chemical Vapor Deposition of Palladium-Platinum Bilayer Nano-Films on Polysulfone. Chinese Journal of Catalysis, 2007, 28, 755-757.	14.0	2
110	Controlled synthesis of truncated octahedral bismuth micron particles with giant positive magnetoresistance. CrystEngComm, 2015, 17, 7056-7062.	2.6	2
111	Synthesis, Characterization and Catalytic Applications in Propane Dehydrogenation of Ordered Mesoporous Alumina. Journal of Nanoscience and Nanotechnology, 2009, 9, 6876-82.	0.9	1
112	Reinjection flow field-flow fractionation method for nanoparticle quantitative analysis in unknown and complex samples. Journal of Chromatography A, 2021, 1638, 461897.	3.7	1
113	Large-Scale Synthesis of a Novel Tri(8-Hydroxyquioline) Aluminum Nanostructure. Journal of Nanoscience and Nanotechnology, 2006, 6, 2580-2583.	0.9	Ο
114	Electrochemical Treatment of Reverse Osmosis Concentrate of Oil Refining Wastewater by Mn-Sn-Ce/gamma-Al2O3 Particle Electrode. , 2012, , .		0
115	Current Water Treatment Technologies: An Introduction. , 2021, , 1-35.		Ο
116	Application of Heterogeneous Nanocatalysis-Based Advanced Oxidation Processes in Water Purification. , 2021, , 2941-2987.		0
117	Application of Heterogeneous Nanocatalysis-Based Advanced Oxidation Processes in Water Purification. , 2021, , 1-47.		Ο
118	Current Water Treatment Technologies: An Introduction. , 2021, , 2033-2066.		0
119	Current Water Treatment Technologies. , 2020, , 1-47.		0